

Published in final edited form as:

Brain Res. 2011 April 28; 1387: 71–84. doi:10.1016/j.brainres.2011.02.080.

Mesolimbic effects of the antidepressant fluoxetine in Holtzman rats, a genetic strain with increased vulnerability to stress

Eimeira Padilla, Jason Shumake, Douglas W. Barrett, Eva C. Sheridan, and F. Gonzalez-Lima

University of Texas at Austin, Departments of Psychology and Pharmacology, 1 University Station A8000, Austin, TX 78712, USA

Abstract

This is the first metabolic mapping study of the effects of fluoxetine after learned helplessness training. Antidepressants are the most commonly prescribed medications, but the regions underlying treatment effects in affectively disordered brains are poorly understood. We hypothesized the antidepressant action of fluoxetine would produce adaptations in mesolimbic regions after two weeks of treatment. We used Holtzman rats, a genetic strain showing susceptibility to novelty-evoked hyperactivity and stress-evoked helplessness, to map regional brain metabolic effects caused by fluoxetine treatment. Animals underwent learned helplessness, and subsequently immobility time was scored in the forced swim test (FST). On the next day, animals began receiving two weeks of fluoxetine (5 mg/kg/day) or vehicle and were retested in the FST at the end of drug treatment. Antidepressant behavioral effects of fluoxetine were analyzed using a ratio of immobility during pre- and post-treatment FST sessions. Brains were analyzed for regional metabolic activity using quantitative cytochrome oxidase histochemistry as in our previous study using congenitally helpless rats. Fluoxetine exerted a protective effect against FST-induced immobility behavior in Holtzman rats. Fluoxetine also caused a significant reduction in the mean regional metabolism of the nucleus accumbens shell and the ventral hippocampus as compared to vehicle-treated subjects. Additional networks affected by fluoxetine treatment included the prefrontal-cingulate cortex and brainstem nuclei linked to depression (e.g. habenula, dorsal raphe and interpeduncular nucleus). We concluded that corticolimbic regions such as the prefrontal-cingulate cortex, nucleus accumbens, ventral hippocampus and key brainstem nuclei represent important contributors to the neural network mediating fluoxetine antidepressant action.

Keywords

Cytochrome oxidase; Brain mapping; Depression; Fluoxetine; Antidepressant effect; Animal model

1. Introduction

In 2005, antidepressants surpassed antihypertensive agents as the most commonly prescribed class of medications in office-based and hospital outpatient-based medical practice (Olfson

© 2011 Elsevier B.V. All rights reserved.

Corresponding author: Prof. Dr. F. Gonzalez-Lima, University of Texas at Austin, 1 University Station A8000, Austin, TX 78712, Tel.: +1 (512) 471-5895; Fax: +1 (512) 471-4728, gonzalez-lima@mail.utexas.edu.

Publisher's Disclaimer: This is a PDF file of an unedited manuscript that has been accepted for publication. As a service to our customers we are providing this early version of the manuscript. The manuscript will undergo copyediting, typesetting, and review of the resulting proof before it is published in its final citable form. Please note that during the production process errors may be discovered which could affect the content, and all legal disclaimers that apply to the journal pertain.

and Marcus, 2009). Depression and anxiety disorders such as post-traumatic stress disorder (PTSD) are most commonly treated with selective serotonin reuptake inhibitor (SSRI) antidepressants, of which fluoxetine is the prototypical drug (Devane et al., 2005; Hemels et al., 2002; Olfson and Marcus, 2009). However, not much is known regarding the neural regions that underlie treatment response, which usually requires several weeks before efficacy is observed. Increased knowledge of the regions affected after two weeks of antidepressant treatment can aid in the understanding of neural networks underlying the initial response to fluoxetine. Notably, metabolic activity changes in the prefrontal cortex and subgenual cingulate (known as infralimbic cortex in rodents) could predict a response to fluoxetine in depressed patients (Mayberg et al., 2000). While PET and fMRI imaging have been used to examine the effects of antidepressants in humans, it is difficult to resolve small subcortical structures, such as the nucleus accumbens, which is also involved in antidepressant action (Shirayama and Chaki, 2006). Metabolic mapping techniques in animals are useful tools for studying the functional effects of antidepressant treatment because they have the spatial resolution to implicate individual subcortical nuclei that cannot be detected with human neuroimaging methods.

In the present study, we examined fluoxetine effects in the rat brain using quantitative cytochrome oxidase histochemistry and interregional brain activity correlations in order to extend the map of the neural network underlying antidepressant response to subcortical nuclei (Gonzalez-Lima and Cada, 1998). Cytochrome oxidase is the terminal respiratory enzyme in the mitochondrial electron transport chain that is correlated to ATP synthesis and serves as an endogenous metabolic marker for neuronal functional activity (Wong-Riley, 1989). In addition, cytochrome oxidase is a long-term indicator of brain metabolic capacity (Wong-Riley et al., 1998), making histochemical quantification of cytochrome oxidase activity an ideal marker for examining the long-lasting effects of antidepressant treatment on regional brain metabolism (Gonzalez-Pardo et al., 2008; Nobrega et al., 1993; O'Reilly et al., 2009; Shumake et al., 2010).

In animals, the Porsolt forced swim test (FST) has been used extensively as a model of behavioral despair (Porsolt et al., 1978). In this model, rodents are subjected to inescapable stress, and depressive-like behavior is characterized by increased floating behavior or immobility (Porsolt et al., 1978). Treatment with standard antidepressant drugs can decrease FST immobility (Cryan et al., 2005; Porsolt et al., 1978), an effect correlated with antidepressant efficacy in humans (Detke et al., 1995; Porsolt et al., 1977). Decreased immobility in FST has correlated to treatment efficacy between different types of antidepressant drugs including fluoxetine (Porsolt et al., 1978; Porsolt et al., 1979). In the present study, the antidepressant-like effects of two weeks of daily fluoxetine treatment were examined by comparing ratios of immobility between pre- and post-treatment FST sessions. A two-week course of fluoxetine was chosen to examine the relatively early antidepressant effects on brain and behavior (Shumake et al., 2010).

The effects of fluoxetine treatment on regional brain metabolism have been previously analyzed using deoxyglucose uptake in normal rats (Freo et al., 2000; Jang et al., 2009). However, fluoxetine may influence affectively disordered brains differently than normal brains. We recently examined the effects associated with two weeks of fluoxetine on FST-induced immobility and on changes in regional cytochrome oxidase activity in naïve congenitally helpless rats, a selectively bred line of Sprague-Dawley rats (Shumake et al., 2010). Congenitally helpless rats have innate brain alterations such as a hypermetabolic habenula and hypometabolic ventral tegmental area, and may show spontaneous helpless behavior in the absence of learned helplessness training (Shumake and Gonzalez-Lima, 2003). These innate metabolic alterations and the FST immobility scores were improved in congenitally helpless rats following two weeks of 5 mg/kg/day fluoxetine. In the present

study, the regional brain effects of the same 2-week fluoxetine antidepressant treatment were investigated with a different rat strain, the Holtzman rats. This is a genetic strain that exhibits a bipolar behavioral phenotype, characterized by novelty-induced hyperactivity and stress-induced depressive behavior (Padilla et al., 2009; Padilla et al., 2010; Spivey et al., 2008; Wieland et al., 1986), similar to that found in bipolar depression. Furthermore, we wanted to characterize the behavior of Holtzman rats using the FST and the learned helplessness behavioral paradigms to determine the correlative relationship between these two models of depression.

One previous study examined the effects of acute fluoxetine injections on brain deoxyglucose uptake in Sprague-Dawley rats and on their behavioral response in the FST, but they did not examine the nucleus accumbens (Jang et al., 2009), a region with relevance to depression and antidepressant action (Shirayama and Chaki, 2006). To our knowledge, the brain effects of chronic fluoxetine have not been investigated before in Holtzman subjects. Therefore, we wished to determine whether administration of fluoxetine to Holtzman rats would affect brain regions similar to those implicated in depression neuroimaging studies.

2. Results

2.1. Learned helplessness does not correlate with forced swim behavior in Holtzman rats

Before drug treatment all subjects received the same behavioral training and testing. As listed in Table 1, subjects were handled and tested for learned helplessness in a shuttle box. Subjects were then matched based on their learned helplessness scores (escape latencies) and assigned to either fluoxetine or vehicle groups. Latency to escape shock in the learned helplessness test was not correlated with immobility time in the FST prior to antidepressant treatment ($p > 0.1$). Since there were no correlations between behavioral paradigms, we continued to investigate the effects of fluoxetine treatment using the forced swim test.

2.2. Confirmation of fluoxetine antidepressant behavioral effects in Holtzman rats

There were no significant differences in escape latencies (FR1 jump or FR2 latencies, $p > 0.5$) between the groups of rats chosen for drug or vehicle treatment. The immobility of rats analyzed before and after two weeks of fluoxetine (5 mg/kg/day i.p.) treatment showed evidence of antidepressant effects in the FST. A FST-induced immobility ratio was computed between pre- and post-drug treatment and it was termed the FST treatment response ratio, with higher values indicating a greater therapeutic response to fluoxetine (i.e. less immobility in the post-treatment session). The FST response ratios were normally distributed; therefore a univariate ANOVA was performed with FST response ratio as the dependent variable and treatment as the independent variable. One subject was an outlier (defined as more than 3 standard deviations over the mean) and was excluded from the analysis resulting in a total of 34 subjects (fluoxetine $n = 18$, vehicle $n = 16$). There was a treatment effect in which fluoxetine significantly increased the FST response ratio ($p = 0.003$) (Table 2).

2.3. Fluoxetine reduced mean cytochrome oxidase in the nucleus accumbens shell and ventral hippocampus in Holtzman rats

Cytochrome oxidase activity was sampled from 41 regions (Figure 1) selected based on previous research by our lab (Shumake et al., 2000; Shumake et al., 2004; Shumake and Gonzalez-Lima, 2003) and neuroimaging studies showing fluoxetine treatment effects (Freo et al., 2008; Mayberg et al., 1999; Mayberg et al., 2000). The only significant mean regional differences in cytochrome oxidase activity between fluoxetine-treated subjects and vehicle-treated subjects were in the shell of the nucleus accumbens and in the ventral hippocampus

(CA3 field) ($p < 0.05$). No other significant mean regional differences were found between fluoxetine-treated subjects and vehicle-treated subjects. To determine whether fluoxetine treatment produced any general effects on brain metabolism, the cytochrome oxidase measurements from all regions were averaged for fluoxetine and vehicle-treated groups. There was no significant difference on overall brain metabolic activity ($p = 0.70$). Means and standard errors for all regions of interest are reported in Table 3.

2.4. Prefrontal cortical interregional correlations in fluoxetine and vehicle-treated groups

The large, rich datasets derived from the regional metabolic mapping allowed the measurement of cortical and subcortical regions in fluoxetine and vehicle-treated subjects. This afforded the capability to evaluate not only mean cytochrome oxidase activity changes but also the covariance relationships between the activities of regions throughout the brain (Puga et al., 2007). Particularly striking were the observed patterns of activity inter-correlations among cortical regions implicated in depressive behavior. Table 4 compares interregional correlations of the prefrontal cortical regions in fluoxetine and vehicle-treated subjects. Within-group pair-wise correlations significantly different from zero are indicated by asterisks, and between-groups significant differences are boldfaced. Briefly, we found that fluoxetine increased negative correlations between the anterior cingulate cortex and ventromedial prefrontal regions, and reduced the correlations between the infralimbic and all other prefrontal cortical regions. There was a remarkable increased differentiation in the correlations between prefrontal regions in the fluoxetine group in comparison to the vehicle-treated group, which showed positive correlations among prefrontal regions, except in the anterior cingulate cortex, which was decoupled from other prefrontal regions. The most significant findings were that the cingulate cortex showed negative functional correlations to ventromedial prefrontal regions (medial orbital and prelimbic cortices) and the infralimbic cortex changed from being highly positively correlated with other prefrontal cortical regions (dorsal frontal, lateral frontal, anterior insular, lateral orbital, medial orbital, and prelimbic cortices) in the vehicle-treated group to being uncorrelated in the fluoxetine group.

2.5. Cortical-subcortical inter-correlations in fluoxetine and vehicle-treated groups

Most notably, fluoxetine treatment increased the functional correlations between the prefrontal cortex and the hippocampus. Prefrontal regions (insular, orbital and prelimbic cortices) showed strong functional correlations with hippocampal regions in the fluoxetine group (positive as well as negative correlations), as opposed to weaker correlations in the vehicle group (Table 5). Other significant group differences can be summarized as follows:

1. Habenula activity showed strong positive correlations with prefrontal regions (dorsal, orbital and prelimbic cortices) in the fluoxetine group as opposed to weaker negative correlations present in the vehicle group.
2. Medial septal activity showed a positive correlation to the dorsal prefrontal cortex and a weak positive correlation to the medial orbital cortex among the vehicle group. In contrast, the medial septum was weakly negatively correlated to the dorsal frontal and negatively correlated with the medial orbital cortex among the fluoxetine group.
3. Interpeduncular nucleus activity was positively correlated to the lateral orbital cortex among the fluoxetine-treated and these regions were decoupled among the vehicle-treated subjects.
4. Finally, activity in the core of the nucleus accumbens was decoupled from the anterior cingulate superficial cortical layers among the fluoxetine-treated rats and these regions were correlated among the vehicle-treated animals

2.6. Subcortical inter-correlations in fluoxetine and vehicle-treated groups

Fluoxetine treatment changed the direction and magnitude of the activity correlations between regions in the habenula-raphé-interpeduncular network. The most interesting group differences were in the interregional correlations between the dorsal raphe, habenula, and interpeduncular nucleus network (Table 6). The dorsal raphe was strongly negatively correlated to the habenula among the vehicle group as opposed to the weaker positive correlations observed in the fluoxetine group. Furthermore, the dorsal raphe was decoupled from the interpeduncular nucleus in the vehicle group and strongly positively correlated to this region in the fluoxetine group. Other significant group differences can be summarized as follows:

1. Activity in the lateral habenula showed strong negative correlations with the interpeduncular nucleus among the vehicle group versus positive correlations in the fluoxetine group.
2. Lateral septal activity was strongly positively correlated to regions of the ventral striatum (accumbens core and ventral pallidum) in the vehicle group and was decoupled from these regions in the fluoxetine group.
3. Activity in the interpeduncular nucleus was strongly positively correlated to the dorsal hippocampus among fluoxetine-treated subjects, in contrast to the decoupling observed in the vehicle group.
4. Activity in the interpeduncular nucleus was positively correlated with the medial amygdala in the fluoxetine group and weakly negatively correlated in the vehicle group.
5. Finally, correlations between subregions of the hippocampal formation were greater among the fluoxetine group (r 's range: 0.80 to 0.92) versus the vehicle group (r 's range: 0.14 to 0.63).

3. Discussion

The major effects caused by two weeks of fluoxetine (5 mg/kg/day) in Holtzman rats may be summarized as follows: 1) Fluoxetine exerted a protective effect against stress-induced depressive-like behavior in the forced swim test. 2) Fluoxetine caused a significant reduction in the mean regional metabolism of the nucleus accumbens shell and ventral hippocampus as compared to vehicle-treated subjects. 3) Fluoxetine treatment reduced activity inter-correlations within the prefrontal cortex regions while increasing inter-correlations between the prefrontal cortex and the anterior cingulate cortex and hippocampus. 4) Finally, fluoxetine treatment changed the direction and magnitude of the activity inter-correlations between regions in the habenula-raphé-interpeduncular nucleus network.

3.1. Learned helplessness escape scores were not correlated with forced swim immobility

The Porsolt forced swim test (FST) has been used extensively as a model of behavioral despair. In this model, animals are subjected to inescapable stress and depressive-like behavior is characterized by increased floating-behavior or immobility (Porsolt et al., 1978). Inescapable stress is a common factor in the learned helplessness and forced swim paradigms; however, another study also reported that forced swim behavior was not correlated with shuttle box escape responses (Drugan et al., 1989). Drugan et al. (1989) showed that there was stability within each behavioral stress paradigm, i.e. there was a high correlation within shuttle box escape behavior and within the forced swim test when animals were retested using the same paradigm 2 and 4 weeks later. However, when subjects underwent the learned helplessness paradigm and then performed the forced swim test, there was no correlation. Possible explanations by the authors included that animals show different

distributions of responses between each paradigm. Specifically, the shuttle box-escape task has a bimodal distribution in which subjects' responses fall into one of two categories – failure or success. On the other hand, the forced swim test produces a unimodal, graded continuum of immobility scores (Drugan et al., 1989). This has also been the case with our subjects in which shuttle box behavior fall into one of two clusters – helpless or non-helpless (Padilla et al., 2009; Padilla et al., 2010). However, the forced swim test immobility time is normally distributed and unimodal (data not shown). Drugan et al. (1989) also proposed that the models are not predictive of one another because 1) the observed correlation within models represents an artifact of training or a memory effect that is not seen between models and 2) different neurochemical mechanisms may be responsible for the stress-induced behavioral deficits in these models. Together with our study, these data suggest that forced swim behavior is not well correlated with shuttle box escape responding.

3.2. Effect of fluoxetine on FST-induced immobility

Previous studies have repeatedly shown that treatment with standard antidepressant drugs, including selective serotonin reuptake inhibitors (SSRIs), can block FST-induced immobility in rodents (Cryan et al., 2005; Detke et al., 1997; Porsolt et al., 1977). As a result, the FST is considered a useful screening tool for new antidepressant compounds (Porsolt et al., 1977; Porsolt et al., 1978). Unlike Detke et al. (1997), we did not find a significant effect of fluoxetine treatment on absolute immobility scores during the post-treatment FST, only a trend in this direction. However, given that we had performed a complete two-session FST before treatment, we were able to use a pre-drug measure of immobility to evaluate post-drug treatment response for individual subjects and thereby increase statistical power to detect treatment effects. Using this novel measure we observed that fluoxetine-treated individuals showed greater improvement between the second sessions of the pre- and post-treatment FST. This antidepressant effect was not present when the first sessions of the pre- and post-treatment FST were compared. This supports the idea that the first session of the FST does not reveal antidepressant effects, and also rules out non-specific motor activation effects of fluoxetine treatment. Furthermore, our results suggest that exposure to inescapable forced swim stress followed by a test session 24 hours later is an important determinant in the reinstatement of helpless behavior and observation of a drug treatment effect. Based on these results, the behavioral improvement observed was likely due to an antidepressant effect which supported the use of Holtzman rats to characterize the neural regions underlying fluoxetine treatment effects.

3.3. Reduction of nucleus accumbens and ventral hippocampal metabolism produced by fluoxetine

The only mean regional effects caused by two weeks of fluoxetine (5 mg/kg/day) were decreases in cytochrome oxidase activity in the nucleus accumbens shell and the ventral hippocampus CA3. Reduced metabolism in the ventral hippocampus is consistent with extensive research demonstrating the role of this region in stress, emotion and affect (Fanselow and Dong, 2010). In fact, lesions to the ventral hippocampus, and not the dorsal hippocampus, reduced fear expression and blunted the neuroendocrine stress response in rats (Kjelstrup et al., 2002).

The nucleus accumbens was also the region with the largest decrease in cytochrome oxidase activity in a study with another antidepressant, amitriptyline, used in conjunction with an inhibitory avoidance learning experiment (Gonzalez-Pardo et al., 2008). Interestingly, decreased expression of D2 dopamine receptors, due to chronic mild stress, was reported in the nucleus accumbens shell and core (Dziedzicka-Wasylewska et al., 1997). Antidepressant treatment using imipramine or fluoxetine reversed the reduction of D2 receptor mRNA in the shell, but not in the core (Dziedzicka-Wasylewska et al., 1997). Using a genetic rat

model of depression (Flinders sensitive line or FSL rats), investigators reported changes in serotonin turnover only in the nucleus accumbens after chronic desipramine treatment (Zangen et al., 1997). Notably, the change in serotonin levels was not affected by desipramine in control Sprague-Dawley rats. Together with our results, these data suggest that stress-induced changes in the nucleus accumbens are more responsive to antidepressant treatment. Moreover, deep brain stimulation of the nucleus accumbens had significant antidepressant effects in a population of patients with severe treatment resistant depression (Bewernick et al., 2010). Notably, the Bewernick et al. (2010) study targeting the accumbens with DBS found no long-term effects (neither an increase or decrease) in accumbens metabolism as measured by PET, but manipulating this region did evoke metabolic changes in an associated network involving the subgenual cingulate and orbital prefrontal cortex. Others have found that DBS causes local disruption of neuronal activity while at the same time activating networked regions via white matter projections (Hamani et al., 2010; Mayberg et al., 2005).

Congenitally helpless rats selectively bred from Sprague-Dawley rats did not show a modification in nucleus accumbens metabolism after the same fluoxetine treatment. Instead, they showed increased metabolic activity in the ventral tegmental area, and reduced metabolism in the habenula, dorsal dentate gyrus and dorsomedial prefrontal cortex (Shumake et al., 2010). Another study observed that 2 weeks of fluoxetine treatment reduced glucose metabolism in the lateral habenula and the dorsal hippocampus CA3 field (Freo et al., 2000). The discrepant findings could be due to an interaction with stress (learned helplessness and multiple FST) which was reduced or absent in previous studies looking at the simple metabolic effects of chronic fluoxetine treatment. Despite this difference, the regions affected by fluoxetine treatment are limited to the mesolimbic network. Antidepressant treatment may have diverse effects on this network, which may fluctuate depending on the presence of external stressors and the characteristics of the population affected. These individual differences are also present in humans and probably underlie the disparities observed in neuroimaging studies of depression (Rigucci et al., 2010; Trivedi et al., 2008).

3.4. Fluoxetine increases inter-correlations of prefrontal regions with the cingulate cortex and reduces inter-correlations of the infralimbic cortex with other prefrontal regions

Functional connectivity is a specific term defined in metabolic mapping studies and refers to activity inter-correlations or coupling among regions (covariate measure), different from mean regional activity (univariate measure) (Anand et al., 2005; McIntosh and Gonzalez-Lima, 1994; Morris et al., 1999). Fluoxetine increased negative coupling between anterior cingulate cortex and ventromedial prefrontal cortex, and reduced positive coupling between the infralimbic cortex and other prefrontal regions. Both the anterior cingulate and infralimbic cortex (subgenual anterior cingulate cortex in humans) appear to play major roles in antidepressant treatment (Rigucci et al., 2010). For example, antidepressant treatments increase corticolimbic functional connectivity between the anterior cingulate and limbic regions among depressed patients (Anand et al., 2005). In addition, increased metabolic activity in the dorsolateral prefrontal cortex coupled with reduction in ventral limbic regions, including the subgenual cingulate, is associated with an antidepressant response after 6 weeks of SSRI treatment among depressed patients (Goldapple et al., 2004; Mayberg et al., 2000).

Furthermore, the infralimbic cortex is a therapeutic target for treatment-resistant depression. In previous human and rodent studies, lesions or electrical stimulation of this area (thought to suppress local neural activity) have produced antidepressant effects (Cosgrove and Rauch, 1995; Hamani et al., 2010; Lozano et al., 2008). A dissociation of this ventral limbic area from dorsal cortical structures may represent a unique treatment effect. In human studies,

limbic-cortical dysregulation has been proposed as a network model for depression and is characterized by dorsal cortical hypoactivity with hyperactive ventral limbic areas in humans (Mayberg, 1997). The question remains as to why we did not observe mean differences in these regions as predicted by human studies. One possible explanation is that two regions can show changes in covariance without a significant change in regional activity (McIntosh and Gonzalez-Lima, 1994), and behavioral-related plasticity may first involve a change in covariances between neural elements, which then leads to a change in mean regional activity (Ahissar et al., 1992). Since single brain regions do not operate in isolation of each other, increased differentiation of the inter-correlations with the prefrontal network may be more representative of the brain mechanism underlying a therapeutic response.

3.5. Fluoxetine increased functional connectivity of the prefrontal-hippocampal network

Fluoxetine-treated subjects had increased functional connectivity between the prefrontal cortex (especially the medial orbital and prelimbic cortices) and the hippocampus, and also displayed greater intra-hippocampal connectivity. This network has been extensively implicated in the pathophysiology of depression. The literature has implicated reduced hippocampal volume (Bremner et al., 2000; Sheline et al., 1996) and decreased hippocampal neurogenesis in the effects of depression (Elder et al., 2006; Paizanis et al., 2007). However, antidepressant-induced changes in hippocampal function have rarely been assessed with functional neuroimaging. Our findings are consistent with previous reports of reciprocal metabolic changes in the prefrontal-hippocampal network after antidepressant treatment in depressed patients (Delaveau et al., 2010). For example, Kennedy et al. (2001) observed that after successful paroxetine therapy in depressed humans, increased glucose metabolism occurred in dorsolateral, ventrolateral, and medial aspects of the prefrontal cortex, coupled with decreased metabolism in hippocampal and parahippocampal regions (Kennedy et al., 2001).

3.6. The dorsal raphe, habenula, and interpeduncular nucleus as an important subcortical network for fluoxetine effects

These subcortical regions have well defined anatomical interconnections. The dorsal raphe projects to the habenula (Lowry et al., 2008). The lateral habenula sends projections to the dorsal raphe (Aghajanian and Wang, 1977). The medial habenula sends most of its fibers to the interpeduncular nucleus (Contestabile and Flumerfelt, 1981; Herkenham and Nauta, 1979) and also sends axonal projections to the lateral habenula (Kim and Chang, 2005). Finally, the interpeduncular nucleus sends projections to the dorsal raphe (Shibata and Suzuki, 1984). Interestingly, both the habenula and dorsal raphe have been linked to human depression and hypersensitivity to stress in animals (Grahn et al., 1999; Hikosaka et al., 2008; Morris et al., 1999; Shumake and Gonzalez-Lima, 2003). Increased activity in the habenula is related to depressive-like behavior in numerous studies (Caldecott-Hazard et al., 1988; Morris et al., 1999; Rosier et al., 2009; Shumake et al., 2003). For example, patients experiencing transient depressive episodes elicited by acute tryptophan depletion showed increased blood flow or metabolism in the habenula that correlate with ratings of depressed mood and inversely with plasma tryptophan levels (Morris et al., 1999; Rosier et al., 2009).

The medial and lateral habenula receive input from other regions of the limbic system (e.g. prelimbic cortex, septum, hypothalamus, preoptic area, nucleus of the diagonal band) and the lateral habenula projects to regions such as the ventral tegmental area and dorsal raphe (Hikosaka et al., 2008; Vertes, 2004). This positions the habenula in a critical role as mediator of the interactions that occur between limbic regions and other nuclei that have previously been linked to depression and anxiety. For example, serotonin (5HT) neurons within the dorsal raphe are normally under autoinhibitory control of 5HT_{1A} somatodendritic receptors (Cooper et al., 2003). The 5HT_{1A} autoreceptors are especially susceptible to

desensitization produced by high levels of extracellular 5HT which occur after exposure to inescapable stress (Maier and Watkins, 2005). Desensitization of 5HT_{1A} autoreceptors and increased 5HT release from the dorsal raphe appear necessary for the development of learned helplessness (Grahn et al., 1999; Maier et al., 1993; Petty et al., 1994), and the habenula plays an important role in mediating increased dorsal raphe activity in response to inescapable stress (Amat et al., 2001). In fact, lesioning the habenula can prevent the rise in serotonin release from the dorsal raphe following inescapable shock and blocks the development of learned helplessness (Amat et al., 2001). Therefore, the observed switching from a strong negative inter-correlation of activity to a weaker positive one between the lateral habenula and dorsal raphe may represent a unique fluoxetine effect associated with an antidepressant response.

Another network difference that distinguished the fluoxetine-treated from the vehicle group was the strong positive correlations between the interpeduncular nucleus, the dorsal raphe, and the habenula. The interpeduncular nucleus receives more acetylcholine input than any other region in the mammalian brain (Woolf and Butcher, 1985), and there is evidence that excessive cholinergic activity is implicated in the etiology of depression (Charles et al., 1994; Dilsaver and Coffman, 1989; Janowsky et al., 1983; Steingard et al., 2000). The amygdala, which is also part of the mesolimbic neurocircuitry of stress and fear (Shin and Liberzon, 2010), showed a positive correlation with the interpeduncular nucleus in the fluoxetine group as opposed to a weaker negative correlation in the vehicle group. Fluoxetine-induced changes in the covariance between the interpeduncular nucleus and subcortical nuclei such as the dorsal raphe, habenula and amygdala could represent another potential mechanism underlying treatment effects.

In conclusion, this study is unique because it is the first to characterize the metabolic differences and network effects of 2-week fluoxetine treatment in both subcortical nuclei and cortical regions among susceptible rodents after learned helplessness training. The nucleus accumbens and ventral hippocampus were the only regions showing mean differences in our study, which is interesting in light of recent findings showing that deep brain stimulation of the nucleus accumbens had significant antidepressant effects in patients with treatment resistant depression (Bewernick et al., 2010) and lesions specific to the ventral hippocampus can reduce anxiety in rats (Kjelstrup et al., 2002). Our functional connectivity findings also suggest that the nucleus accumbens, hippocampus, infralimbic cortex and key brainstem nuclei may provide important contributions to the neural network mediating fluoxetine antidepressant action.

4. Experimental procedures

4.1. Animals

We used 55 young adult male Holtzman rats from Harlan (Madison, WI), housed 2–3 per cage and maintained on a 12h/12h light/dark photoperiod in a facility accredited by the Association for the Assessment of Laboratory Animal Care International. 35 rats were used as subjects for the behavioral experiments and fluoxetine/vehicle treatment, and 20 rats were used to obtain brain homogenate standards for quantitative cytochrome oxidase histochemistry. Food and water were available *ad libitum*. Experiments occurred during the light phase between 0700 h and 1900 h. Prior to the start of experiments, subjects were handled and weighed for five minutes every day for one week. The rats were 45 days old at the start of behavioral experiments. Drug treatment began at 50 days old, and post-treatment FST sessions and brain tissue collection occurred at 78 days old, which constitutes young adulthood (Farris, 1942) (Table 1). Procedures were done in accordance with NIH guidelines and approved by the Institutional Animal Care and Use Committee.

4.2. Apparatus

For learned helplessness training, rats were placed first in a chamber for delivery of inescapable shocks, and the following day in a shuttle box where they could escape from the shocks. The inescapable shock chambers (30 cm × 25 cm × 20 cm) (Med Associates, St. Albans, VT) were enclosed in sound-attenuated boxes and illuminated by a red light. The apparatus had two sides of aluminum, with clear plexiglass for the front, back, and top. A soapy solution of Ivory dishwashing liquid (Procter and Gamble, Cincinnati, OH) was placed in the tray beneath the chambers to provide a distinct olfactory cue for the inescapable context. Shocks were delivered through metal bars separated by 1.2 cm forming the floor of the chamber, which was wired to shock generators (Med Associates). The chamber was controlled by MED-PC, version 4 (Med Associates, St. Albans, VT), using a program written in the MEDSTATE language.

The shuttle box (42 cm × 16 cm × 25 cm) consisted of two compartments of equal size, separated by a door (11 cm × 9 cm) that remained open throughout the session. The shuttle box was enclosed in a sound-attenuated box and illuminated by a white light (10 lx). Two sides of the shuttle box were aluminum, with clear plexiglass for the front, back, and top. Shocks were delivered through metal bars separated by 1.2 cm forming the floor of the shuttle box, which was wired to shock generators (Med Associates). The subject's position was detected by eight sets of infrared light beam motion detectors, located 2 cm above the grid floor, spaced 4.4 cm apart from each other, on both sides of the shuttle box. The shuttle box was controlled by MED-PC, version 4, using a program written in the MEDSTATE language. This program used beam breaks of the two pairs of beams located at either end of both sides of the shuttle box as the contingency for terminating shock, to score a complete crossing. A povidone-iodine solution (First Priority, INC., Elgin, IL) was placed in the tray beneath the shuttle box to provide a distinct olfactory cue.

For the forced swim test (FST), rats were placed in a clear acrylic cylinder (50.8 cm in height by 21.6 cm in diameter) filled to 37.1 cm with 25°C water. After the FST, the rats were removed from the water, dried with towels, and placed in a cage on top of a heating pad for 30 min. The cylinders were emptied and cleaned between rats.

4.3. Behavioral procedures

Experiments lasted 28 days as listed in Table 1. Learned helplessness training took place after six days of handling, on the seventh and eighth days. On the seventh day, subjects were trained in the inescapable shock chamber to induce the helpless phenotype (Overmier and Seligman, 1967). Each session included 60 trials of 10 s duration 1.0 mA shocks. Pseudorandom inter-trial intervals consisted of durations ranging from 10 to 110 seconds. On the eighth day, subjects were tested with the escapable shock paradigm using a shuttle box to measure escape behavior (Padilla et al., 2009). Briefly, subjects were tested with a fixed ratio (FR) 1 schedule consisting of jumping or running from one side of the box to the other to terminate the shock. In the FR2 schedule, animals had to cross twice; in other words, rats had to run back to the compartment where the shock was initiated in order to escape the shock. This escape contingency was done for 25 trials and required more time to complete; therefore if the subject failed to perform the appropriate response, the shock automatically terminated after 30 seconds. FR1 jump and FR1/FR2 run were performed to determine the optimum contingency for measuring learned helplessness (Hunziker and Dos Santos, 2007). Latency to escape was automatically scored using MED-PC software.

On the tenth and eleventh days, animals were evaluated for depressive-like behavior with a pre-drug forced swim test (FST). Briefly, the FST is a 2-day procedure (2 sessions) in which rats swim under conditions in which they cannot escape (Porsolt et al., 1977). On the first

FST day, the rats are forced to swim for 15 min (Pre-drug FST Session 1). The rats initially struggle to escape from the water, but they eventually adopt a posture of immobility in which they make only the movements necessary to keep their heads above water. When subjects are retested 24 hours later, immobility is increased. Therefore, 24 hours later rats were retested under identical swim conditions for 5 min (Pre-drug FST Session 2). Both of the forced swimming sessions were videotaped from the side of the cylinders and scored by raters unaware of the treatment condition. Immobility time was defined as the time in which the rat remained in a stationary posture that did not reflect attempts to escape from the water. In this characteristic posture, the forelimbs are motionless and tucked toward the body. A rat was judged to be immobile if it was making only movements necessary to keep its head above water. The forced swim test is used to measure depressive-like behavior and it is sensitive to the effects of antidepressants such as tricyclic antidepressants (TCAs) and selective serotonin reuptake inhibitors (SSRIs) which decrease immobility (Detke et al., 1995; Porsolt et al., 1977; Porsolt et al., 1978). Subjects repeated two FST sessions at the end of drug treatment (Post-drug FST).

On the twelfth day, the learned helplessness scores were used to divide the subjects into two groups matched by their escape latencies. One group was treated with fluoxetine and another group with vehicle for 14 days (Days 12–26). Fluoxetine hydrochloride (Spectrum Chemicals, Gardena, CA) was reconstituted using a dimethylsulfoxide (DMSO) / normal saline vehicle (25/75 percent) to make a 2.5 mg/ml fluoxetine solution. Fluoxetine (5 mg/kg) or vehicle (25% DMSO / 75% normal saline) was administered intraperitoneally (i.p.) once a day for two weeks beginning one day after the pre-drug FST Session 2. We chose to study two-week drug effects because in depressed humans the therapeutic response to antidepressant drugs does not occur after acute administration, but rather emerges slowly over the course of weeks. Although acute administration of SSRIs can improve FST performance, this occurs at high doses (≥ 20 mg/kg) (Bianchi et al., 2002; Dow et al., 2005; Jang et al., 2009) that are well above clinically effective doses for humans. However, Detke, Johnson, and Lucki (1997) showed that a lower dose of fluoxetine (5 mg/kg) is effective in the FST when given chronically (daily injections for 2 weeks) (Detke et al., 1997).

On Day 26, animals were retrained in the forced swim cylinder for 15 min and then received the last fluoxetine dose (Post-drug FST Session 1). Twenty-four hours later (Day 27), rats were re-tested in the FST for 5 min (Post-drug FST Session 2). Individual differences in immobility scores between the 5-min sessions of pre-drug (Day 11) and post-drug (Day 27) forced swim tests were used to evaluate the antidepressant effects of fluoxetine treatment.

4.4. Quantitative histochemistry

Following decapitation on Day 28, brains were removed and frozen rapidly in isopentane. Using a cryostat (Reichert-Jung) at -20 °C, brains were sectioned at 40 μ m and kept frozen at -40 °C until they were processed using quantitative cytochrome oxidase histochemistry, as described previously (Gonzalez-Lima and Cada, 1998). Briefly, the procedure involved a series of chemical exposures, the first of which (0.1 M phosphate buffer with 10% wt/vol sucrose and 0.5% vol/vol glutaraldehyde, pH 7.6, for 5 min) facilitated tissue adherence to the slides. The next series of exposures (four changes of 0.1 M phosphate buffer with 10% wt/vol sucrose, for 5 min each) removed red blood cells. Then slides underwent metal intensification (0.05 M Tris buffer, pH 7.6, with 275 mg/l cobalt chloride, 10% wt/vol sucrose, and 0.5% vol/vol dimethylsulfoxide, for 10 min) followed by incubation (350 mg diaminobenzidine tetrahydrochloride, 52.5 mg cytochrome c, 35 g sucrose, 14 mg catalase, and 1.75 ml dimethylsulfoxide in 700 ml of oxygen-saturated 0.1 M phosphate buffer, at 37 °C for 1 h). The reaction was stopped by fixing the tissue (30 min at room temperature with 10% wt/vol sucrose and 4% vol/vol formalin). Finally, slides were dehydrated in ethanol

baths (increasing from 30% to 100% vol/vol ethanol), cleared with xylene, and coverslipped with Permount.

To quantify enzymatic activity and to control for staining variability across different batches of cytochrome oxidase staining, sets of brain tissue-homogenate standards were included with each batch of slides. The enzymatic activity of cytochrome oxidase in this homogenate was assayed using spectrophotometry, as described by Gonzalez-Lima and Cada (1998), and activity units were defined at pH 7 and 37 °C, where 1 unit oxidizes 1 μ mol of reduced cytochrome c per min (μ mol/min/g tissue wet weight). Activity values from the spectrophotometry were assigned to each standard, and calibrated to corresponding optical density measurements of the sections. The resulting linear regression equations ($r^2 > 0.9$) were used to convert optical density readings from brain regions of interest into cytochrome oxidase activity values.

Using an image-processing system (JAVA, Jandel Scientific, Corte Madera, CA), optical density was sampled from every region of interest (Figure 1). Cytochrome oxidase-stained frontal cortical regions showed differences in labeling between the outer superficial half (s = up to layer III) and the inner deeper half (d = layers IV–VI) and thus both superficial (s) and deep (d) halves were analyzed separately. The 41 regions investigated were the prelimbic, dorsal frontal, lateral frontal, anterior insular, lateral orbital, medial orbital, infralimbic, and anterior cingulate cortices, lateral septum, medial septum, nucleus accumbens shell and core, ventral pallidum, medial habenula, lateral habenula, dorsal and ventral subiculum, dentate gyrus, and hippocampus (CA1, CA2, and CA3), retrosplenial cortex, periaqueductal gray, interpeduncular nucleus, ventral tegmental area, dorsal raphe nucleus and amygdala (central, medial and basolateral nuclei). The sampling window was adjusted for each region so that it was as large as possible while still allowing for four, non-overlapping readings to be taken bilaterally from each region. In addition, each region was sampled from three different sections per animal, and these readings were averaged in order to obtain representative values for each region for each subject. Sample sizes varied across regions because the relevant tissue from some subjects was lost or damaged during sectioning and histochemical staining.

4.5. Statistical analyses

All statistics were computed using SPSS (v. 11.0). A ratio of immobility time during pre-drug and post-drug treatment FST 5-min sessions was calculated and termed the FST treatment response ratio. This ratio standardized differences in immobility that were present before drug treatment. Regional mean differences in cytochrome oxidase activity between fluoxetine and vehicle-treated groups were evaluated using one-way ANOVA. Pearson product-moment correlations of cytochrome oxidase activity between all measured regions were calculated for each group (within-group analysis). A jackknife procedure was performed in which each individual subject was dropped from a group, and then correlations were calculated again without that subject's data. This procedure was iterated until each subject had been sequentially dropped and the analysis repeated. To minimize Type I error, correlations that remained significantly different from zero at $p < 0.05$ through all iterations were considered statistically reliable for further analysis. These correlations were then tested for significant differences between groups (between-group analysis). The Fisher Z transformation was used to convert each correlation to a Z score to test differences in interregional correlations between groups (Bruchey and Gonzalez-Lima, 2006; Jones and Gonzalez-Lima, 2001; Puga et al., 2007). The significant between-group interregional correlations were verified with bootstrap using R statistical software version 2.9.0. The term functional connection or functional coupling was used to refer to a significant activity correlation between two brain regions.

Acknowledgments

We thank Bailey Kermath, Jennifer Lynn Krüg, Dr. Julio C. Rojas, Dr. Jaclyn M. Spivey, Dr. Penny D. Riha and Dr. Aleksandra K. Bruchey for their technical assistance and feedback. This work was supported by NIH grant R01 MH076847 to FGL and T32 MH65728 fellowships to EP and JS. Dr. Padilla conducted this study in partial fulfillment of the requirements for the Ph.D. degree at the University of Texas at Austin.

Reference List

- Aghajanian GK, Wang RY. Habenular and other midbrain raphe afferents demonstrated by a modified retrograde tracing technique. *Brain Res.* 1977; 122:229–242. [PubMed: 837230]
- Ahissar E, Vaadia E, Ahissar M, Bergman H, Arieli A, Abeles M. Dependence of cortical plasticity on correlated activity of single neurons and on behavioral context. *Science.* 1992; 257:1412–1415. [PubMed: 1529342]
- Amat J, Sparks PD, Matus-Amat P, Griggs J, Watkins LR, Maier SF. The role of the habenular complex in the elevation of dorsal raphe nucleus serotonin and the changes in the behavioral responses produced by uncontrollable stress. *Brain Res.* 2001; 917:118–126. [PubMed: 11602236]
- Anand A, Li Y, Wang Y, Wu J, Gao S, Bukhari L, Mathews VP, Kalnin A, Lowe MJ. Antidepressant effect on connectivity of the mood-regulating circuit: an FMRI study. *Neuropsychopharmacology.* 2005; 30:1334–1344. [PubMed: 15856081]
- Bewernick BH, Hurlmann R, Matusch A, Kayser S, Grubert C, Hadrysiewicz B, Axmacher N, Lemke M, Cooper-Mahkorn D, Cohen MX, Brockmann H, Lenartz D, Sturm V, Schlaepfer TE. Nucleus accumbens deep brain stimulation decreases ratings of depression and anxiety in treatment-resistant depression. *Biol. Psychiatry.* 2010; 67:110–116. [PubMed: 19914605]
- Bianchi M, Moser C, Lazzarini C, Vecchiato E, Crespi F. Forced swimming test and fluoxetine treatment: in vivo evidence that peripheral 5-HT in rat platelet-rich plasma mirrors cerebral extracellular 5-HT levels, whilst 5-HT in isolated platelets mirrors neuronal 5-HT changes. *Exp. Brain Res.* 2002; 143:191–197. [PubMed: 11880895]
- Bremner JD, Narayan M, Anderson ER, Staib LH, Miller HL, Charney DS. Hippocampal volume reduction in major depression. *Am. J. Psychiatry.* 2000; 157:115–118. [PubMed: 10618023]
- Bruchey AK, Gonzalez-Lima F. Brain activity associated with fear renewal. *Eur. J. Neurosci.* 2006; 24:3567–3577. [PubMed: 17229105]
- Caldecott-Hazard S, Mazziotta J, Phelps M. Cerebral correlates of depressed behavior in rats, visualized using 14C-2-deoxyglucose autoradiography. *J. Neurosci.* 1988; 8:1951–1961. [PubMed: 3385484]
- Charles HC, Lazeyras F, Krishnan KR, Boyko OB, Payne M, Moore D. Brain choline in depression: in vivo detection of potential pharmacodynamic effects of antidepressant therapy using hydrogen localized spectroscopy. *Prog. Neuropsychopharmacol. Biol. Psychiatry.* 1994; 18:1121–1127. [PubMed: 7846284]
- Contestabile A, Flumerfelt BA. Afferent connections of the interpeduncular nucleus and the topographic organization of the habenulo-interpeduncular pathway: an HRP study in the rat. *J. Comp Neurol.* 1981; 196:253–270. [PubMed: 7217357]
- Cooper, JR.; Bloom, FE.; Roth, RH. Serotonin, Histamine and Adenosine. In: Cooper, JR.; Bloom, FE.; Roth, RH., editors. *The biochemical basis of neuropharmacology.* Oxford: Oxford University Press; 2003. p. 271-304.
- Cosgrove GR, Rauch SL. Psychosurgery. *Neurosurg. Clin. N. Am.* 1995; 6:167–176. [PubMed: 7696872]
- Cryan JF, Valentino RJ, Lucki I. Assessing substrates underlying the behavioral effects of antidepressants using the modified rat forced swimming test. *Neurosci. Biobehav. Rev.* 2005; 29:547–569. [PubMed: 15893822]
- Delaveau P, Jabourian M, Lemogne C, Guionnet S, Bergouignan L, Fossati P. Brain effects of antidepressants in major depression: A meta-analysis of emotional processing studies. *Journal of Affective Disorders.* 2010

- Detke MJ, Johnson J, Lucki I. Acute and chronic antidepressant drug treatment in the rat forced swimming test model of depression. *Exp. Clin. Psychopharmacol.* 1997; 5:107–112. [PubMed: 9234045]
- Detke MJ, Rickels M, Lucki I. Active behaviors in the rat forced swimming test differentially produced by serotonergic and noradrenergic antidepressants. *Psychopharmacology (Berl.)*. 1995; 121:66–72. [PubMed: 8539342]
- Devane CL, Chiao E, Franklin M, Kruep EJ. Anxiety disorders in the 21st century: status, challenges, opportunities, and comorbidity with depression. *Am. J. Manag. Care.* 2005; 11:S344–S353. [PubMed: 16236016]
- Dilsaver SC, Coffman JA. Cholinergic hypothesis of depression: a reappraisal. *J. Clin. Psychopharmacol.* 1989; 9:173–179. [PubMed: 2661605]
- Dow AL, Russell DS, Duman RS. Regulation of activin mRNA and Smad2 phosphorylation by antidepressant treatment in the rat brain: effects in behavioral models. *J. Neurosci.* 2005; 25:4908–4916. [PubMed: 15901772]
- Drugan RC, Skolnick P, Paul SM, Crawley JN. A pretest procedure reliably predicts performance in two animal models of inescapable stress. *Pharmacol. Biochem. Behav.* 1989; 33:649–654. [PubMed: 2587607]
- Dziedzicka-Wasylewska M, Willner P, Papp M. Changes in dopamine receptor mRNA expression following chronic mild stress and chronic antidepressant treatment. *Behav. Pharmacol.* 1997; 8:607–618. [PubMed: 9832973]
- Elder GA, De Gasperi R, Gama Sosa MA. Research update: neurogenesis in adult brain and neuropsychiatric disorders. *Mt. Sinai J. Med.* 2006; 73:931–940. [PubMed: 17195878]
- Fanselow MS, Dong HW. Are the dorsal and ventral hippocampus functionally distinct structures? *Neuron.* 2010; 65:7–19. [PubMed: 20152109]
- Farris, EJ. Breeding of the Rat. In: Griffith, JQ.; Farris, EJ., editors. *The Rat in Laboratory Investigation*. Philadelphia: J.B. Lippincott Company; 1942. p. 1-17.
- Freo U, Merico A, Ermani M, Ori C. Cerebral metabolic effects of fluoxetine, fluvoxamine, paroxetine and sertraline in the conscious rat. *Neurosci. Lett.* 2008; 436:148–152. [PubMed: 18387742]
- Freo U, Ori C, Dam M, Merico A, Pizzolato G. Effects of acute and chronic treatment with fluoxetine on regional glucose cerebral metabolism in rats: implications for clinical therapies. *Brain Res.* 2000; 854:35–41. [PubMed: 10784104]
- Goldapple K, Segal Z, Garson C, Lau M, Bieling P, Kennedy S, Mayberg H. Modulation of cortical-limbic pathways in major depression: treatment-specific effects of cognitive behavior therapy. *Arch. Gen. Psychiatry.* 2004; 61:34–41. [PubMed: 14706942]
- Gonzalez-Lima, F.; Cada, A. Quantitative histochemistry of cytochrome oxidase activity: theory, methods, and regional brain vulnerability. In: Gonzalez-Lima, F., editor. *Cytochrome oxidase in neuronal metabolism and Alzheimer's disease*. New York: Plenum Press; 1998. p. 55-90.
- Gonzalez-Pardo H, Conejo NM, Arias JL, Monleon S, Vinader-Caerols C, Parra A. Changes in brain oxidative metabolism induced by inhibitory avoidance learning and acute administration of amitriptyline. *Pharmacol. Biochem. Behav.* 2008; 89:456–462. [PubMed: 18313125]
- Grahn RE, Will MJ, Hammack SE, Maswood S, McQueen MB, Watkins LR, Maier SF. Activation of serotonin-immunoreactive cells in the dorsal raphe nucleus in rats exposed to an uncontrollable stressor. *Brain Res.* 1999; 826:35–43. [PubMed: 10216194]
- Hamani C, Diwan M, Macedo CE, Brandao ML, Shumake J, Gonzalez-Lima F, Raymond R, Lozano AM, Fletcher PJ, Nobrega JN. Antidepressant-like effects of medial prefrontal cortex deep brain stimulation in rats. *Biol. Psychiatry.* 2010; 67:117–124. [PubMed: 19819426]
- Hemels ME, Koren G, Einarson TR. Increased use of antidepressants in Canada: 1981–2000. *Ann. Pharmacother.* 2002; 36:1375–1379. [PubMed: 12196054]
- Herkenham M, Nauta WJ. Efferent connections of the habenular nuclei in the rat. *J. Comp Neurol.* 1979; 187:19–47. [PubMed: 226566]
- Hikosaka O, Sesack SR, Lecourtier L, Shepard PD. Habenula: crossroad between the basal ganglia and the limbic system. *J. Neurosci.* 2008; 28:11825–11829. [PubMed: 19005047]
- Hunziker MH, Dos Santos CV. Learned helplessness: effects of response requirement and interval between treatment and testing. *Behav. Processes.* 2007; 76:183–191. [PubMed: 17540513]

- Jang DP, Lee SH, Park CW, Lee SY, Kim YB, Cho ZH. Effects of fluoxetine on the rat brain in the forced swimming test: a [F-18]FDG micro-PET imaging study. *Neurosci. Lett.* 2009; 451:60–64. [PubMed: 19110032]
- Janowsky DS, Risch SC, Gillin JC. Adrenergic-cholinergic balance and the treatment of affective disorders. *Prog. Neuropsychopharmacol. Biol. Psychiatry.* 1983; 7:297–307. [PubMed: 6684317]
- Jones D, Gonzalez-Lima F. Mapping Pavlovian conditioning effects on the brain: blocking, contiguity, and excitatory effects. *J. Neurophysiol.* 2001; 86:809–823. [PubMed: 11495952]
- Kennedy SH, Evans KR, Kruger S, Mayberg HS, Meyer JH, McCann S, Arifuzzman AI, Houle S, Vaccarino FJ. Changes in regional brain glucose metabolism measured with positron emission tomography after paroxetine treatment of major depression. *Am. J. Psychiatry.* 2001; 158:899–905. [PubMed: 11384897]
- Kim U, Chang SY. Dendritic morphology, local circuitry, and intrinsic electrophysiology of neurons in the rat medial and lateral habenular nuclei of the epithalamus. *J. Comp Neurol.* 2005; 483:236–250. [PubMed: 15678472]
- Kjelstrup KG, Tuvnes FA, Steffenach HA, Murison R, Moser EI, Moser MB. Reduced fear expression after lesions of the ventral hippocampus. *Proc. Natl. Acad. Sci. U. S. A.* 2002; 99:10825–10830. [PubMed: 12149439]
- Lowry CA, Hale MW, Evans AK, Heerkens J, Staub DR, Gasser PJ, Shekhar A. Serotonergic systems, anxiety, and affective disorder: focus on the dorsomedial part of the dorsal raphe nucleus. *Ann. N. Y. Acad. Sci.* 2008; 1148:86–94. [PubMed: 19120094]
- Lozano AM, Mayberg HS, Giacobbe P, Hamani C, Craddock RC, Kennedy SH. Subcallosal cingulate gyrus deep brain stimulation for treatment-resistant depression. *Biol. Psychiatry.* 2008; 64:461–467. [PubMed: 18639234]
- Maier SF, Grahn RE, Kalman BA, Sutton LC, Wiertelak EP, Watkins LR. The role of the amygdala and dorsal raphe nucleus in mediating the behavioral consequences of inescapable shock. *Behav. Neurosci.* 1993; 107:377–388. [PubMed: 8484901]
- Maier SF, Watkins LR. Stressor controllability and learned helplessness: the roles of the dorsal raphe nucleus, serotonin, and corticotropin-releasing factor. *Neurosci. Biobehav. Rev.* 2005; 29:829–841. [PubMed: 15893820]
- Mayberg HS. Limbic-cortical dysregulation: a proposed model of depression. *J. Neuropsychiatry Clin. Neurosci.* 1997; 9:471–481. [PubMed: 9276848]
- Mayberg HS, Brannan SK, Tekell JL, Silva JA, Mahurin RK, McGinnis S, Jerabek PA. Regional metabolic effects of fluoxetine in major depression: serial changes and relationship to clinical response. *Biol. Psychiatry.* 2000; 48:830–843. [PubMed: 11063978]
- Mayberg HS, Liotti M, Brannan SK, McGinnis S, Mahurin RK, Jerabek PA, Silva JA, Tekell JL, Martin CC, Lancaster JL, Fox PT. Reciprocal limbic-cortical function and negative mood: converging PET findings in depression and normal sadness. *Am. J. Psychiatry.* 1999; 156:675–682. [PubMed: 10327898]
- Mayberg HS, Lozano AM, Voon V, McNeely HE, Seminowicz D, Hamani C, Schwalb JM, Kennedy SH. Deep brain stimulation for treatment-resistant depression. *Neuron.* 2005; 45:651–660. [PubMed: 15748841]
- McIntosh AR, Gonzalez-Lima F. Structural equation modeling and its application to network analysis in functional brain imaging. *Human Brain Mapping.* 1994; 2:2–22.
- Morris JS, Smith KA, Cowen PJ, Friston KJ, Dolan RJ. Covariation of activity in habenula and dorsal raphe nuclei following tryptophan depletion. *Neuroimage.* 1999; 10:163–172. [PubMed: 10417248]
- Nobrega JN, Raymond R, DiStefano L, Burnham WM. Long-term changes in regional brain cytochrome oxidase activity induced by electroconvulsive treatment in rats. *Brain Res.* 1993; 605:1–8. [PubMed: 8385539]
- O'Reilly KC, Shumake J, Bailey SJ, Gonzalez-Lima F, Lane MA. Chronic 13-cis-retinoic acid administration disrupts network interactions between the raphe nuclei and the hippocampal system in young adult mice. *Eur. J. Pharmacol.* 2009; 605:68–77. [PubMed: 19168052]
- Olfson M, Marcus SC. National patterns in antidepressant medication treatment. *Arch. Gen. Psychiatry.* 2009; 66:848–856. [PubMed: 19652124]

- Overmier JB, Seligman ME. Effects of inescapable shock upon subsequent escape and avoidance responding. *J. Comp Physiol Psychol.* 1967; 63:28–33. [PubMed: 6029715]
- Padilla E, Barrett D, Shumake J, Gonzalez-Lima F. Strain, sex, and open-field behavior: factors underlying the genetic susceptibility to helplessness. *Behav. Brain Res.* 2009; 201:257–264. [PubMed: 19428642]
- Padilla E, Shumake J, Barrett DW, Holmes G, Sheridan E, Gonzalez-Lima F. Novelty-evoked activity in open field predicts susceptibility to helpless behavior. *Physiol Behav.* 2010 in press.
- Paizanis E, Hamon M, Lanfumey L. Hippocampal neurogenesis, depressive disorders, and antidepressant therapy. *Neural Plast.* 2007; 2007:73754. [PubMed: 17641737]
- Petty F, Kramer G, Wilson L, Jordan S. In vivo serotonin release and learned helplessness. *Psychiatry Res.* 1994; 52:285–293. [PubMed: 7991722]
- Porsolt RD, Anton G, Blavet N, Jalfre M. Behavioural despair in rats: a new model sensitive to antidepressant treatments. *Eur. J. Pharmacol.* 1978; 47:379–391. [PubMed: 204499]
- Porsolt RD, Bertin A, Blavet N, Deniel M, Jalfre M. Immobility induced by forced swimming in rats: effects of agents which modify central catecholamine and serotonin activity. *Eur. J. Pharmacol.* 1979; 57:201–210. [PubMed: 488159]
- Porsolt RD, Le Pichon M, Jalfre M. Depression: a new animal model sensitive to antidepressant treatments. *Nature.* 1977; 266:730–732. [PubMed: 559941]
- Puga F, Barrett DW, Bastida CC, Gonzalez-Lima F. Functional networks underlying latent inhibition learning in the mouse brain. *Neuroimage.* 2007; 38:171–183. [PubMed: 17703956]
- Rigucci S, Serafini G, Pompili M, Kotzalidis GD, Tatarelli R. Anatomical and functional correlates in major depressive disorder: the contribution of neuroimaging studies. *World J. Biol. Psychiatry.* 2010; 11:165–180. [PubMed: 19670087]
- Rosier JP, Levy J, Fromm SJ, Nugent AC, Talagala SL, Hasler G, Henn FA, Sahakian BJ, Drevets WC. The effects of tryptophan depletion on neural responses to emotional words in remitted depression. *Biol. Psychiatry.* 2009; 66:441–450. [PubMed: 19539268]
- Sheline YI, Wang PW, Gado MH, Csernansky JG, Vannier MW. Hippocampal atrophy in recurrent major depression. *Proc. Natl. Acad. Sci. U. S. A.* 1996; 93:3908–3913. [PubMed: 8632988]
- Shibata H, Suzuki T. Efferent projections of the interpeduncular complex in the rat, with special reference to its subnuclei: a retrograde horseradish peroxidase study. *Brain Res.* 1984; 296:345–349. [PubMed: 6704742]
- Shin LM, Liberzon I. The neurocircuitry of fear, stress, and anxiety disorders. *Neuropsychopharmacology.* 2010; 35:169–191. [PubMed: 19625997]
- Shirayama Y, Chaki S. Neurochemistry of the nucleus accumbens and its relevance to depression and antidepressant action in rodents. *Curr. Neuropharmacol.* 2006; 4:277–291. [PubMed: 18654637]
- Shumake J, Colorado RA, Barrett DW, Gonzalez-Lima F. Metabolic mapping of the effects of the antidepressant fluoxetine on the brains of congenitally helpless rats. *Brain Res.* 2010; 1343:218–225. [PubMed: 20470763]
- Shumake J, Conejo-Jimenez N, Gonzalez-Pardo H, Gonzalez-Lima F. Brain differences in newborn rats predisposed to helpless and depressive behavior. *Brain Res.* 2004; 1030:267–276. [PubMed: 15571675]
- Shumake J, Edwards E, Gonzalez-Lima F. Opposite metabolic changes in the habenula and ventral tegmental area of a genetic model of helpless behavior. *Brain Res.* 2003; 963:274–281. [PubMed: 12560133]
- Shumake J, Gonzalez-Lima F. Brain systems underlying susceptibility to helplessness and depression. *Behav. Cogn Neurosci. Rev.* 2003; 2:198–221. [PubMed: 15006293]
- Shumake J, Poremba A, Edwards E, Gonzalez-Lima F. Congenital helpless rats as a genetic model for cortex metabolism in depression. *Neuroreport.* 2000; 11:3793–3798. [PubMed: 11117493]
- Spivey J, Barrett D, Padilla E, Gonzalez-Lima F. Mother-infant separation leads to hypoactive behavior in adolescent Holtzman rats. *Behav. Processes.* 2008; 79:59–65. [PubMed: 18585869]
- Steingard RJ, Yurgelun-Todd DA, Hennen J, Moore JC, Moore CM, Vakili K, Young AD, Katic A, Beardslee WR, Renshaw PF. Increased orbitofrontal cortex levels of choline in depressed adolescents as detected by in vivo proton magnetic resonance spectroscopy. *Biol. Psychiatry.* 2000; 48:1053–1061. [PubMed: 11094138]

- Trivedi MH, Hollander E, Nutt D, Blier P. Clinical evidence and potential neurobiological underpinnings of unresolved symptoms of depression. *J. Clin. Psychiatry*. 2008; 69:246–258. [PubMed: 18363453]
- Vertes RP. Differential projections of the infralimbic and prelimbic cortex in the rat. *Synapse*. 2004; 51:32–58. [PubMed: 14579424]
- Wieland S, Boren JL, Consroe PF, Martin A. Stock differences in the susceptibility of rats to learned helplessness training. *Life Sci*. 1986; 39:937–944. [PubMed: 3489150]
- Wong-Riley M, Anderson B, Liebl W, Huang Z. Neurochemical organization of the macaque striate cortex: correlation of cytochrome oxidase with Na+K+ATPase, NADPH-diaphorase, nitric oxide synthase, and N-methyl-D-aspartate receptor subunit 1. *Neuroscience*. 1998; 83:1025–1045. [PubMed: 9502244]
- Wong-Riley MT. Cytochrome oxidase: an endogenous metabolic marker for neuronal activity. *Trends Neurosci*. 1989; 12:94–101. [PubMed: 2469224]
- Wolf NJ, Butcher LL. Cholinergic systems in the rat brain: II. Projections to the interpeduncular nucleus. *Brain Res. Bull*. 1985; 14:63–83. [PubMed: 2580607]
- Zangen A, Overstreet DH, Yadid G. High serotonin and 5-hydroxyindoleacetic acid levels in limbic brain regions in a rat model of depression: normalization by chronic antidepressant treatment. *J. Neurochem*. 1997; 69:2477–2483. [PubMed: 9375680]

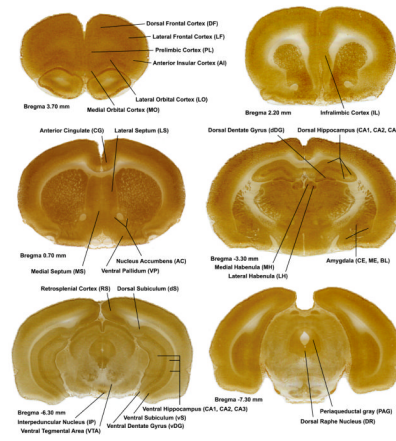


Figure 1. Coronal rat brain sections. Each image is a coronal brain section histochemically stained for cytochrome oxidase activity, and depicting regions of interest by Bregma level. Anterior–posterior Bregma coordinates are indicated below each image.

Table 1

Experimental procedures and days performed.

Procedure	Day
Handle	1 – 6
Inescapable footshock (60 trials)	7
Shuttle box escape (FR1/FR2 trials)	8
Pre-drug FST session 1 (15 min)	10
Pre-drug FST session 2 (5 min)	11
Fluoxetine/vehicle treatment (2 weeks)	12 – 26
Post-drug FST session 1 (15 min)	26
Post-drug FST session 2 (5 min)	27
Tissue processing	28

Table 2

Means analysis of immobility in the FST between fluoxetine and vehicle groups.

FST 5-minute session	Fluoxetine (n=18) Mean \pm SE	Vehicle (n=16) Mean \pm SE
Immobility pre-treatment (sec)	78.6 \pm 9.9	61.5 \pm 10.2
Immobility post-treatment (sec)	62.9 \pm 7.4	71.9 \pm 7.5
Immobility ratio pre/post-treatment	1.26 \pm 0.09 *	0.83 \pm 0.11

* $p < 0.01$, fluoxetine versus vehicle.

Table 3

Means and standard errors (S.E.) of cytochrome oxidase activity (micromole/minute/gram wet tissue) of regions of interest in fluoxetine-treated and vehicle groups.

Brain Region	Abbrev.	Fluoxetine (n) Mean \pm S.E.	Vehicle (n) Mean \pm S.E.
Accumbens shell	ACs	220.1 \pm 5.9 (16) *	239.2 \pm 6.9 (16)
Accumbens core	ACc	211.9 \pm 6.4 (16)	229.6 \pm 8.9 (16)
Dorsal dentate gyrus	dDG	309.1 \pm 10.9 (14)	295.2 \pm 8.7 (11)
Dorsal hippocampus CA1	dCA1	222.4 \pm 6.1 (14)	213.1 \pm 4.7 (11)
Dorsal hippocampus CA2	dCA2	244.9 \pm 8.7 (14)	235.0 \pm 7.2 (11)
Dorsal hippocampus CA3	dCA3	217.1 \pm 6.5 (14)	206.9 \pm 4.0 (11)
Dorsal subiculum	dS	234.1 \pm 7.0 (17)	238.1 \pm 4.7 (17)
Ventral dentate gyrus	vDG	305.9 \pm 11.0 (16)	314.5 \pm 7.8 (17)
Ventral hippocampus CA1	vCA1	249.8 \pm 7.7 (17)	252.1 \pm 3.8 (17)
Ventral hippocampus CA2	vCA2	268.2 \pm 7.9 (17)	267.2 \pm 4.7 (17)
Ventral hippocampus CA3	vCA3	245.2 \pm 2.4 (16) *	253.3 \pm 2.4 (17)
Ventral subiculum	vS	323.7 \pm 6.8 (17)	324.14 \pm 4.8 (17)
Medial septum	MS	185.2 \pm 6.9 (16)	185.5 \pm 4.6 (16)
Lateral septum	LS	242.0 \pm 7.4 (16)	256.6 \pm 6.7 (16)
Medial habenula	MH	272.8 \pm 8.6 (14)	263.4 \pm 9.5 (12)
Lateral habenula	LH	322.5 \pm 9.0 (14)	316.90 \pm 7.3 (12)
Dorsal raphe	DR	240.5 \pm 6.7 (12)	252.4 \pm 8.4 (12)
Interpeduncular nucleus	IP	387.0 \pm 11.6 (15)	378.1 \pm 7.4 (13)
Periaqueductal gray	PAG	264.8 \pm 7.4 (12)	267.9 \pm 8.6 (12)
Ventral pallidum	VP	224.0 \pm 5.4 (18)	236.5 \pm 5.8 (16)
Ventral tegmental area	VTA	186.0 \pm 13.4 (16)	181.3 \pm 7.2 (13)
Central amygdala	CE	257.6 \pm 5.7 (14)	252.3 \pm 4.7 (11)
Medial amygdala	ME	250.4 \pm 9.9 (14)	243.9 \pm 4.3 (11)
Basolateral amygdala	BL	267.8 \pm 7.2 (14)	266.6 \pm 3.7 (11)
Infralimbic cortex superficial	ILs	241.7 \pm 3.9 (17)	252.8 \pm 6.3 (15)
Infralimbic cortex deep	ILd	250.4 \pm 3.3 (17)	258.9 \pm 6.6 (15)
Prelimbic cortex superficial	PLs	235.8 \pm 3.3 (12)	235.5 \pm 4.8 (12)
Prelimbic cortex deep	PLd	239.8 \pm 4.3 (12)	243.9 \pm 7.1 (12)
Dorsal frontal superficial	DFs	242.1 \pm 6.0 (12)	238.7 \pm 7.9 (12)
Dorsal frontal deep	DFd	252.3 \pm 7.9 (12)	251.0 \pm 7.6 (12)
Lateral frontal superficial	LFs	233.9 \pm 5.1 (12)	237.8 \pm 6.6 (12)
Lateral frontal deep	LFd	237.0 \pm 4.8 (12)	237.5 \pm 6.3 (12)
Anterior insular cortex superficial	AI _s	215.4 \pm 2.0 (12)	216.8 \pm 4.3 (12)
Anterior insular cortex deep	AI _d	225.8 \pm 2.1 (12)	225.1 \pm 5.7 (12)
Lateral orbital cortex superficial	LO _s	243.0 \pm 5.3 (12)	243.3 \pm 6.6 (12)
Lateral orbital cortex deep	LO _d	241.3 \pm 3.8 (12)	242.4 \pm 5.7 (12)
Medial orbital cortex superficial	MO _s	242.8 \pm 4.7 (12)	241.5 \pm 5.8 (12)
Medial orbital cortex deep	MO _d	240.5 \pm 2.9 (12)	239.9 \pm 4.7 (12)

Brain Region	Abbrev.	Fluoxetine (n) Mean ± S.E.	Vehicle (n) Mean ± S.E.
Anterior cingulate superficial	CGs	258.2 ± 6.0 (16)	269.5 ± 7.3 (16)
Anterior cingulate deep	CGd	236.8 ± 6.6 (16)	247.8 ± 6.2 (16)
Retrosplenial cortex	RS	311.7 ± 8.4 (17)	309.0 ± 5.8 (17)

*
p < 0.05, fluoxetine versus vehicle.

Table 4

Prefrontal interregional correlation coefficients (r). Each cell lists values for fluoxetine group (upper value) and vehicle group (lower value).

	DFs	DFd	LFs	LFd	Als	AId	LOs	LOd	MOs	MOd	PLs	PLd	CGs
DFd	0.92*												
	0.93*												
LFs	0.53*	0.68*											
	0.84*	0.79*											
LFd	0.27	0.46	0.76*										
	0.81*	0.78*	0.97*										
Als	0.16	0.28	0.01	0.00									
	0.60*	0.69*	0.79*	0.81*									
AId	0.05	0.21	0.22	0.12	0.47*								
	0.39	0.52*	0.73*	0.77*	0.90*								
LOs	0.74*	0.72*	0.30	0.16	0.50*	0.37							
	0.81*	0.75*	0.74*	0.73*	0.70*	0.50*							
LOd	0.86*	0.90*	0.44	0.29	0.47*	0.40	0.85*						
	0.82*	0.88*	0.85*	0.87*	0.68*	0.64*	0.70*						
MOs	0.47	0.51*	0.00	-0.02	0.57*	0.49*	0.60*	0.78*					
	0.72*	0.81*	0.69*	0.63*	0.77*	0.65*	0.68*	0.67*					
MOd	0.68*	0.62*	0.25	0.19	-0.01	0.22	0.50*	0.73*	0.63*				
	0.81*	0.90*	0.66*	0.60*	0.57*	0.41	0.67*	0.71*	0.86*				
PLs	0.59*	0.68*	0.55*	0.52*	-0.06	0.40	0.36	0.68*	0.56*	0.86*			
	0.78*	0.87*	0.67*	0.65*	0.60*	0.47	0.57*	0.64*	0.80*	0.91*			

	DFs	DFd	LFs	LFd	AFs	AId	LOs	LOd	MOs	MOd	PLs	PLd	CGs
PLd	0.40	0.60*	0.48*	0.36	0.19	0.55*	0.20	0.57*	0.60*	0.60*	0.86*		
	0.56*	0.72*	0.65*	0.66*	0.73*	0.69*	0.43	0.57*	0.74*	0.71*	0.85*		
CGs	-0.38	-0.32	-0.30	-0.42	-0.08	-0.01	-0.01	-0.29	-0.23	-0.67*	-0.62*	-0.37	
	-0.02	-0.03	0.15	0.08	0.11	0.31	0.00	0.23	0.12	0.00	0.00	0.10	
CGd	-0.38	-0.33	-0.29	-0.36	0.03	-0.09	-0.03	0.35	-0.27	-0.79*	-0.73*	-0.48*	0.91*
	-0.02	-0.01	0.08	0.01	-0.02	0.20	0.02	0.19	0.04	0.01	0.00	0.04	0.95*
ILs	-0.02	0.00	-0.11	-0.02	0.01	0.07	-0.01	0.02	-0.01	0.04	-0.04	-0.12	0.00
	0.58*	0.60*	0.66*	0.72*	0.63*	0.56*	0.53*	0.42	0.45	0.54*	0.71*	0.69*	-0.01
ILd	0.00	-0.03	0.00	0.06	-0.05	0.01	-0.02	-0.01	0.03	0.02	0.00	-0.02	-0.14
	0.80*	0.73*	0.73*	0.77*	0.58*	0.41	0.66*	0.55*	0.48	0.60*	0.69*	0.57*	-0.04

* significantly different from zero, $p < 0.05$; **bold** = significant group difference, $p < 0.05$.

Prefrontal-subcortical interregional correlation coefficients (r). Each cell lists values for fluoxetine group (upper value) and vehicle group (lower value).

Table 5

	DFs	DFd	LFs	LFd	AFs	AFd	LOs	LOd	MOs	MOd	PLs	PLd	CGs
DR	0.01	0.07	-0.02	-0.13	0.02	0.72*	0.05	0.21	0.12	0.08	0.26	0.36	-0.07
	0.01	0.05	-0.02	0.00	-0.04	0.00	0.00	-0.04	-0.02	-0.03	-0.01	0.02	0.01
MH	0.25	0.35	0.27	0.03	-0.08	-0.08	0.09	0.33	0.15	0.66*	0.64*	0.30	-0.23
	0.01	0.01	-0.05	0.00	0.02	0.00	0.07	-0.03	0.01	-0.01	0.03	0.00	-0.07
LH	0.48*	0.58*	0.43	0.18	-0.02	0.11	0.38	0.58*	0.25	0.84*	0.76*	0.40	-0.35
	-0.33	-0.15	-0.32	-0.16	-0.09	-0.07	-0.17	-0.26	-0.26	-0.26	-0.09	-0.08	0.00
IP	0.53*	0.43	0.33	0.17	0.05	0.16	0.65*	0.62*	0.01	0.38	0.35	0.00	0.02
	0.14	0.03	0.00	-0.03	0.00	-0.14	-0.04	0.11	0.10	0.11	-0.02	-0.02	-0.16
LS	-0.18	-0.13	-0.01	-0.15	-0.02	0.00	0.01	-0.22	-0.28	-0.69*	-0.41	-0.18	0.84*
	0.08	0.10	0.28	0.19	0.08	0.10	-0.01	0.23	0.01	0.00	0.00	0.04	0.73*
MS	-0.37	-0.20	-0.13	-0.13	-0.05	0.02	0.02	-0.22	-0.23	-0.57*	-0.40	-0.17	0.48*
	0.62*	0.61*	0.51*	0.45	0.49*	0.17	0.37	0.39	0.38	0.33	0.46	0.39	0.29
ACs	-0.38	-0.44	-0.09	-0.13	-0.30	0.03	-0.41	-0.53*	-0.31	-0.15	-0.05	-0.09	0.36
	-0.03	-0.01	0.02	0.00	0.00	-0.01	0.08	0.05	0.06	0.00	-0.01	-0.04	0.65*
ACc	0.00	-0.05	-0.02	0.02	-0.13	0.01	-0.16	-0.05	-0.01	0.00	0.01	0.04	0.02
	-0.03	0.13	0.12	-0.05	0.22	0.24	-0.03	0.04	0.19	0.01	0.14	0.26	0.68*
dDG	-0.28	-0.46	-0.20	-0.27	-0.50*	-0.90*	-0.58*	-0.72*	-0.84*	-0.32	-0.37	-0.50*	0.00
	-0.15	0.25	-0.19	-0.19	-0.21	-0.39	-0.26	-0.18	0.05	0.25	-0.19	0.12	0.05
dCAI	-0.11	-0.20	0.13	-0.06	0.01	-0.45	-0.44	-0.43	-0.55*	-0.05	-0.04	-0.28	0.04
	-0.01	0.01	-0.37	-0.37	-0.19	-0.38	-0.22	-0.17	0.02	0.00	-0.08	-0.01	0.03
dCA2	-0.19	-0.40	-0.41	-0.50*	0.04	-0.78*	-0.36	-0.55*	-0.78*	-0.42	-0.56*	-0.68*	0.15

	DFs	DFd	LFs	LFd	Als	AId	LOs	LOd	MOs	MOd	PLs	PLd	CGs
	-0.01	-0.01	-0.22	-0.14	-0.08	-0.28	-0.08	-0.07	-0.03	-0.17	-0.04	-0.04	0.00
dCA3	-0.29	-0.55*	-0.56*	-0.73*	-0.02	-0.71*	-0.29	-0.58*	-0.72*	-0.55*	-0.77*	-0.88*	0.23
	0.01	0.10	-0.28	-0.26	-0.12	-0.32	-0.05	-0.28	-0.12	0.15	-0.13	-0.02	-0.04
vDG	-0.13	-0.04	-0.02	0.09	0.00	0.01	-0.11	-0.09	0.00	0.03	0.01	-0.07	0.01
	-0.01	0.00	-0.05	-0.07	-0.01	0.03	-0.01	0.09	-0.05	0.03	-0.03	-0.05	0.08
vCA1	0.19	0.22	0.02	-0.03	-0.11	0.23	-0.07	0.22	0.31	0.51*	0.72*	0.69*	0.00
	0.00	0.05	0.00	0.00	-0.11	0.00	0.00	0.00	-0.06	0.08	0.20	0.07	-0.03
vCA2	-0.09	0.02	0.00	0.08	0.03	0.40	-0.03	0.04	0.25	0.33	0.65*	0.69*	0.00
	-0.01	-0.02	0.00	0.03	-0.01	0.00	0.01	0.06	-0.01	-0.06	0.11	0.21	-0.02
vCA3	0.18	0.25	0.54*	0.43	0.22	0.53*	0.43	0.33	0.13	0.13	0.28	0.19	0.05
	0.15	0.10	-0.03	-0.02	0.00	-0.07	0.01	-0.02	-0.01	0.00	0.00	0.01	0.02
ds	0.37	0.38	0.27	0.03	0.07	0.26	0.15	0.33	0.34	0.54*	0.75*	0.72*	-0.01
	0.30	0.32	0.00	0.02	0.01	-0.04	0.21	0.16	0.01	0.31	0.29	0.01	-0.27
vS	-0.03	-0.15	0.14	0.09	0.14	0.42	0.14	-0.07	0.29	0.19	0.32	0.55*	0.04
	0.38	0.43	0.42	0.47	0.29	0.28	0.27	0.45	0.10	0.30	0.43	0.51*	0.11*

* significantly different from zero, $p < 0.05$; **bold** = significant group difference, $p < 0.05$.

Table 6

Subcortical interregional correlation coefficients (r). Each cell lists values for fluoxetine group (upper value) and vehicle group (lower value).

	DR	MH	LH	IP	LS	dDG	dCA1	dCA2	vCA1	vCA2	dS
MH	0.23										
	-0.60*										
LH	0.17	0.92*									
	-0.88*	0.75*									
IP	0.65*	0.44	0.52*								
	0.00	-0.14	-0.45								
ACs	-0.02	0.01	0.10	-0.04	0.26						
	-0.18	-0.03	0.00	-0.06	0.59*						
ACC	0.01	-0.03	-0.11	0.05	0.01						
	-0.08	-0.01	0.00	-0.18	0.67*						
PAG	0.01	0.02	0.02	0.07	0.03						
	0.61*	-0.80*	-0.61*	-0.05	0.00						
VP	-0.08	-0.04	-0.02	-0.11	0.00						
	-0.08	-0.01	0.00	-0.18	0.63*						
ME	0.00	0.11	0.15	0.52*	-0.01						
	-0.17	0.23	0.48	-0.21	0.02						
dDG	0.04	-0.01	-0.08	0.73*	0.02						
	-0.23	0.14	0.49*	0.01	0.03						
dCA1	0.02	-0.24	-0.19	0.52*	0.00	0.77*					
	0.13	0.00	0.11	-0.13	0.02	0.42					
dCA2	0.08	-0.22	-0.24	0.57*	-0.01	0.86*	0.80*				

	DR	MH	LH	IP	LS	dDG	dCA1	dCA2	vCA1	vCA2	dS
	-0.36	0.40	0.63*	0.04	0.12	0.39	0.22				
dCA3	-0.06	-0.13	0.15	0.50*	0.02	0.81*	0.69*	0.91*			
	-0.01	-0.05	0.31	-0.18	-0.16	0.48	0.45	0.48			
vDG	0.07	-0.11	-0.17	0.14	0.06	-0.01	0.08	0.01			
	0.01	0.00	-0.01	-0.30	0.06	-0.28	0.01	-0.04			
vCA1	0.37	0.27	0.38	0.32	0.00	0.01	0.09	0.09			
	0.06	0.01	0.08	-0.02	-0.21	-0.01	0.18	-0.15			
vCA2	0.48*	0.36	0.39	0.04	0.00	0.00	-0.10	-0.01	0.92*		
	-0.17	0.06	-0.08	-0.41	0.00	-0.08	0.01	0.09	0.63*		
vCA3	0.43	0.27	0.35	0.55*	-0.10	-0.01	0.05	-0.03	0.37	0.26	
	0.16	-0.26	0.00	-0.01	0.04	0.05	0.25	0.37	0.43	0.07	
dS	0.40	0.33	0.41	0.53*	0.00	-0.02	0.10	0.01	0.89*	0.83*	
	0.00	0.00	-0.03	-0.01	-0.36	-0.03	0.13	0.27	0.70*	0.14	
vS	0.33	0.14	0.13	0.17	0.00	0.02	0.16	0.06	0.79*	0.79*	0.82
	0.08	0.00	-0.02	-0.29	0.01	0.00	0.13	-0.05	0.34	0.72*	0.14

* significantly different from zero, $p < 0.05$; **bold** = significant group difference, $p < 0.05$.